Investigation of Particulate Suspensions in Generalised Hydrodynamic Dissipative Particle Dynamics Using a Spring Model

N. Mai-Duy[1,*], T.Y.N. Nguyen[1], K. Le-Cao[2] and N. Phan-Thien[2]
[1] School of Mechanical and Electrical Engineering,
University of Southern Queensland, Toowoomba, QLD 4350, Australia
[2] Department of Mechanical Engineering, Faculty of Engineering,
National University of Singapore, 9 Engineering Drive 1, 117575, Singapore.

Submitted to *Applied Mathematical Modelling*, March 2019; Revised (1), June 2019; Revised (2), July 2019

ABSTRACT: In the DPD simulation of particulate suspensions, the viscosity of the solvent phase is typically estimated by a non-equilibrium approach, where the fluid is subjected to a flow process (a shear flow), and the local stress and shear rate tensors are calculated; the obtained values (shear stress/shear rate) are then used in calculating the particulate fluid rheology, for example the ratio of the suspension to the matrix viscosity (reduced/relative viscosity) for a given volume fraction of the suspended phase. However, when suspended particles are added, an additional length scale is introduced into the solvent system and this may affect the solvent's macroscopic properties. In this study, a particulate suspension is simulated using a spring model, and the solvent's viscosity is estimated taking into account the finite-size effect (i.e., in the generalised hydrodynamic regime, as hydrodynamics of an integrable system) to produce improved results. Furthermore, it is observed that the simulation results are also affected by the repulsion strength and an appropriate high value of this coefficient, where the actual solvent viscosity in the hydrodynamic limit is still kept close to the input viscosity, can lead to a further improvement. New results are presented and compared with existing data.

*Corresponding author E-mail: nam.mai-duy@usq.edu.au, Telephone +61-7-46312748, Fax +61-7-46312529

Keywords: Dissipative particle dynamics (DPD), particulate suspensions, spring model, generalised hydrodynamics, finite-size effects

1 Introduction

Particulate suspensions are widely encountered in natural and industrial processes. They have been intensively investigated, both computationally and experimentally. Particulate suspensions can be characterised by the dependence of their reduced viscosity on the volume fraction and the shear rate, their non-zero normal stress differences which are functions of the Péclet number, and the migration of solid particles from high to low shear rate regions [1].

Generalised hydrodynamics are developed for simple fluids, as a formulation of integrable system [2,3]. Their transport coefficients are no longer constant but are functions that can vary in space and time - they are dependent on the wavelengths and the frequencies of thermal fluctuations occurring at a finite temperature. For fluctuations with long wavelengths and low frequencies, the fluid behaves like a continuum (original hydrodynamics). For fluctuations with small wavelengths (molecular scale), the fluid is described by a system of interacting particles (molecular dynamics). From the momenta and coordinates of particles in the system at equilibrium, the dependence of its viscosity on the wavelength can be found, and an extrapolation is then carried out to obtain the viscosity in the hydrodynamic limit. With the generalised hydrodynamics theory, finite-size effects can be taken into account.

Dissipative Particle Dynamics (DPD) and Smoothed Dissipative Particle Dynamics (sDPD) are popular numerical techniques for probing the behaviour of complex-structure fluids. The latter can be considered as a direct discretisation of the Navier-Stokes equation with the inclusion of thermal fluctuations, while the former is a coarse-grained model. Recent reviews can be found in [4,5,6]. In DPD [7], each DPD particle is supposed to represent a group of molecules, and forces acting on a DPD particle include conservative, dissipative and random forces. The last two forces form a thermostat to keep the mean specific kinetic energy of the

system constant. DPD conserves momentum locally and thus preserves hydrodynamics. In the simulation of suspensions, a solid particle can be modelled by a set of frozen particles [8], a single particle [9,10,11] or a few constrained basic DPD particles (spring model) [12]. With the use of single particles, a suspended particle is defined/modelled as (i) a hard core covered by a soft shell by the inclusion of lubrication and core forces [9,10]; and (ii) a hard sphere by using an exponential potential for the colloid-colloid conservative interactions [11]. In computing the reduced viscosity, the viscosities of the solvent and the suspension are typically calculated by considering a simple shearing flow of the solvent and the suspension separately, respectively, and the reduced viscosity (defined by the ratio of the suspension viscosity to the solvent viscosity) is found. However, for the former, when solid particles are introduced, the solvent's viscosity can vary according to the generalised hydrodynamics theory. In this regard (to take into account the size effect due to the presence of solid particles), we attempt to employ DPD in its generalised hydrodynamic regime [13,14] to compute the solvent's viscosity for a given volume fraction of the suspended phase. A mechanism to approximately estimate the finite size effects (in the context of the spring model) is proposed. Basically, there are two systems of the same base particles, namely a free system and a system with spring constraints as a model for suspension, to be considered. They are all described by the same linear continuum hydrodynamic equations. Due to the spring constraints, the effective length scale of the solvent phase becomes smaller (less than the side of the simulation box), and the viscosity of the constrained system is thus expected to be smaller than that of the free system at a given wavelength/wave number. Based on the difference in the hydrodynamic limit (defined as the limit when the wave number approaches zero), a new length scale of the solvent can be estimated. For the viscosity of the suspension, we are only interested in its values in the hydrodynamic limit, and a non-equilibrium approach (simple shearing) can thus be applied for an efficient estimation.

We also discuss the effect of repulsive forces on the suspension results. In DPD, a repulsive force is introduced partly to prevent particle overlap, and partly to provide a means to control the compressibility of the model fluid independently of the number density, the cut-off radius and the equilibrium temperature (mean specific kinetic energy). It will be shown that an appropriate high value of the repulsion strength can lead to an improvement in the

simulation results compared to the usual case of when water compressibility is enforced.

The remainder of the paper is organised as follows. Brief reviews of the classical and extended forms of DPD are given in Section 2. Section 3 is concerned with generalised hydrodynamics for simple fluids, where the relation between transverse current autocorrelation functions (TCAFs) and the fluid viscosity is briefly summarised. Section 4 is concerned with particulate suspensions with the focus on the estimate of the solvent's viscosity and the effect of the repulsion strength. Section 5 gives some concluding remarks.

2 Dissipative particle dynamics

2.1 Classical form

In the dissipative particle dynamics (DPD) [7], the fluid is modelled by a system of particles undergoing their Newton 2nd law motions:

$$m_i \ddot{\mathbf{r}}_i = m_i \dot{\mathbf{v}}_i = \sum_{j=1, j\neq i}^{N} \left(\mathbf{F}_{ij,C} + \mathbf{F}_{ij,D} + \mathbf{F}_{ij,R} \right), \tag{1}$$

where m_i, $\mathbf{r}_i$ and $\mathbf{v}_i$ represent the mass, position and velocity vectors of a particle $i = 1, \ldots, N$, respectively; N is the total number of DPD particles; the superposed dot denotes a time derivative; and the three forces on the right side of (1) represent a conservative force (subscript C) used to model the local thermodynamics, a dissipative force (subscript D) to model the fluid viscosity and a random force (subscript R) that accounts for Brownian motion,

$$\mathbf{F}_{ij,C} = a_{ij} w_C \mathbf{e}_{ij}, \tag{2}$$

$$\mathbf{F}_{ij,D} = -\gamma w_D \mathbf{e}_{ij} \cdot \mathbf{v}_{ij} \mathbf{e}_{ij}, \tag{3}$$

$$\mathbf{F}_{ij,R} = \sigma w_R \theta_{ij} \mathbf{e}_{ij}. \tag{4}$$

Here, a_{ij}, γ and σ are the amplitudes, and w_C, w_D and w_R the weighting functions, with $\mathbf{e}_{ij} = \mathbf{r}_{ij}/r_{ij}$ the unit vector from particle j to particle i ($\mathbf{r}_{ij} = \mathbf{r}_i - \mathbf{r}_j$, $r_{ij} = |\mathbf{r}_{ij}|$), $\mathbf{v}_{ij} = \mathbf{v}_i - \mathbf{v}_j$ the relative velocity vector and θ_{ij} a Gaussian white noise. In practice, the weighting functions are usually of the form

$$w_C = \left(1 - \frac{r}{r_c}\right), \tag{5}$$

$$w_D = \left(1 - \frac{r}{r_c}\right)^s, \tag{6}$$

where s is a positive value ($s = 2$: standard value and $s = 1/2$: modified value) and r_c the force cut-off radius beyond which the weighting function vanishes. All these interaction forces are pairwise, center-to-center, and zero outside a cutoff radius. The random force cannot be chosen independently to the dissipative force if the specified energy of the system (Boltzmann temperature $k_B T$) is to be maintained, which is the essence of the fluctuation-dissipation theorem. This requires

$$w_R = \sqrt{w_D}, \quad \sigma = \sqrt{2\gamma k_B T}. \tag{7}$$

After tracking the state of the system (positions and velocities), we can define the density and linear momentum of the fluid as

$$\rho(\mathbf{r}, t) = \sum_i \langle m_i \delta(\mathbf{r} - \mathbf{r}_i) \rangle, \quad \rho(\mathbf{r}, t)\, \mathbf{u}(\mathbf{r}, t) = \sum_i \langle m_i \dot{\mathbf{r}}_i \delta(\mathbf{r} - \mathbf{r}_i) \rangle, \tag{8}$$

and it can be shown that

$$\frac{\partial}{\partial t}\rho + \nabla \cdot (\rho \mathbf{u}) = 0, \qquad \nabla = \partial/\partial \mathbf{r}, \tag{9}$$

$$\frac{\partial}{\partial t}(\rho \mathbf{u}) + \nabla \cdot (\rho \mathbf{u}\mathbf{u}) = \nabla \cdot \mathbf{T}, \tag{10}$$

where $\mathbf{T}$ is the stress tensor given by

$$\mathbf{T} = -\frac{1}{V}\left[\sum_i m \mathbf{V}_i \mathbf{V}_i + \frac{1}{2}\sum_i \sum_{j \neq i} \mathbf{r}_{ij} \mathbf{F}_{ij}\right] = -n\left(\langle m \mathbf{V}\mathbf{V} \rangle + \frac{1}{2}\langle \mathbf{r}\mathbf{F} \rangle\right), \tag{11}$$

in which n is the number density of particles, V is the volume of the bin and $\mathbf{V}_i$ is the fluctuation velocity of particle i with respect to the mean field velocity (peculiar velocity), and the angular brackets denote an ensemble average. The first term on the right side of (11) denotes the contribution to the stress from the momentum (kinetic) transfer of DPD particles and the second term from the interparticle forces. Equations (9) and (10) are recognised as the usual conservation laws - the consequence of the mechanics (1). Two important points should be noted: (a) the method is a truly particle-based method in the sense that it guarantees the satisfaction of conservation laws of mass and momentum in the mean; and (b) the stress, as a result of the microstructure specification, can be *a posteriori* determined from the system state.

2.2 Imposition of fluid properties

One main drawback of the classical DPD formulation is that there is no direct link between the DPD input parameters and the macroscopic properties of the fluid. As shown in [15,16], it is possible to directly impose the viscosity and dynamic response of the fluid in the hydrodynamic limit on the DPD system with the dissipative weighting function taken in its generalised form $w_D = (1 - r/r_c)^s$.

One can use two parameters s and γ to match the viscosity and dynamic response

$$\overline{\eta}_D = \eta, \tag{12}$$

$$\frac{\overline{\eta}}{\rho D} = S_c, \quad D = \frac{2\overline{\eta}_K}{\rho}, \quad \overline{\eta} \simeq \overline{\eta}_D, \tag{13}$$

where S_c is the Schmidt number, η the input/specified viscosity, $\overline{\eta}_D$ and $\overline{\eta}_K$ the dissipative and kinetic viscosities predicted by the kinetic theory, and $\overline{\eta} = \overline{\eta}_K + \overline{\eta}_D$. In 3D space, the parameters s and γ take the form

$$s = \frac{-9 + \sqrt{1 + 4C}}{2}, \quad C = \frac{6 S_c m k_B T n^2 r_c^2}{5\eta^2}, \tag{14}$$

$$\gamma = \frac{5\eta(s+1)(s+2)(s+3)(s+4)(s+5)}{16\pi n^2 r_c^5}. \tag{15}$$

Since $s > 0$, it requires

$$\eta < \sqrt{\frac{3S_c m k_B T n^2 r_c^2}{50}} \quad \text{for a given } S_c, \tag{16}$$

$$S_c > \frac{50\eta^2}{3mk_B T n^2 r_c^2} \quad \text{for a given } \eta. \tag{17}$$

In 2D, the two parameters are

$$s = \frac{-7 + \sqrt{1 + 4C}}{2}, \quad C = \frac{3S_c m k_B T n^2 r_c^2}{4\eta^2}, \tag{18}$$

$$\gamma = \frac{4\eta(s+1)(s+2)(s+3)(s+4)}{3\pi n^2 r_c^4}. \tag{19}$$

Since $s > 0$, it requires

$$\eta < \sqrt{\frac{S_c m k_B T n^2 r_c^2}{16}} \quad \text{for a given } S_c, \tag{20}$$

$$S_c > \frac{16\eta^2}{mk_B T n^2 r_c^2} \quad \text{for a given } \eta. \tag{21}$$

3 Transverse current autocorrelation functions (TCAFs)

In generalised hydrodynamics, the transport coefficients are allowed to be functions that can vary in space or in space and time [2,3]. The current density is given by

$$\mathbf{j}(\mathbf{r}, t) = \sum_{j=1}^{N} \mathbf{v}_j \delta(\mathbf{r} - \mathbf{r}_j(t)), \tag{22}$$

where N is the number of particles and subscripts j denote particle number. Since there is no overall motion, $\langle \mathbf{j}(\mathbf{r}, t) \rangle = 0$ ($< \cdot >$ denoted the average operation). Note that the average of $\mathbf{j}(\mathbf{r}, t)$ is the macroscopic (hydrodynamic) variable and $\mathbf{v}$ the microscopic variable. The Fourier transformation of (22) is

$$\mathbf{J}(\mathbf{k}, t) = \int d\mathbf{r} \exp(i\mathbf{k} \cdot \mathbf{r}) \mathbf{j}(\mathbf{r}, t) = \sum_j \mathbf{v}_j(t) \exp(i\mathbf{k} \cdot \mathbf{r}_j(t)). \tag{23}$$

The spatial correlation function is defined as

$$C_{\alpha\beta}(\mathbf{k},t) = \frac{k^2}{N}\langle J_\alpha(-\mathbf{k},0)J_\beta(\mathbf{k},t)\rangle, \tag{24}$$

where α and β denote Cartesian indices.

For an isotropic fluid, the correlation function (24) depends only on the magnitude of $\mathbf{k}$ and one can decompose it into the longitudinal ($_\parallel$) and transverse ($_\perp$) components relative to $\mathbf{k}$ as

$$C_{\alpha\beta}(k,t) = \frac{k_\alpha k_\beta}{k^2}C_\parallel(k,t) + \left(\delta_{\alpha\beta} - \frac{k_\alpha k_\beta}{k^2}\right)C_\perp(k,t), \tag{25}$$

where $\delta_{\alpha\beta}$ is the Kronecker delta, and

$$C_\perp(k,t) = \frac{k^2}{N}\langle J_\perp(-\mathbf{k},0)J_\perp(\mathbf{k},t)\rangle, \tag{26}$$

$$C_\parallel(k,t) = \frac{k^2}{N}\langle J_\parallel(-\mathbf{k},0)J_\parallel(\mathbf{k},t)\rangle. \tag{27}$$

In the case of Newtonian fluids, one has the following relation

$$\frac{C_\perp(k,t)}{C_\perp(k,0)} = \exp\left[-\frac{\eta_k k^2 t}{\rho}\right], \tag{28}$$

from which the viscosity in the Fourier-transformed space can be estimated from equilibrium correlation function data.

4 Particulate suspensions

The solvent phase is modelled with $\eta = 30$ and $S_c = 500$ which correspond to the following DPD parameters:

$$\begin{aligned} a_{ij} &= 3.53, \quad & m &= 1, \\ s &= 0.42, \quad & k_BT &= 1, \\ \gamma &= 6.97, \quad & r_c &= 1.5, \end{aligned} \tag{29}$$

and the number density $n = 4$. Here, r_c is chosen to be greater than 1 in order to produce a large size ratio of the colloidal to the solvent particle [17].

Here, the units of mass, length and energy are respectively chosen as the mass of a single DPD particle ($\overline{m}$), the force cut-off radius divided by 1.5 ($\overline{r}_c/1.5$), and the kinetic energy ($\overline{k_B T}$), where the superposed bar is used to denote a dimensional quantity. The repulsion a_{ij} in (29) is obtained for a liquid with a water-like compressibility [18]. Figure 1 shows the dependence of the solvent's viscosity on the wave number k ($k = 2\pi/\lambda$, λ: the wavelength). Components of $\mathbf{k}$ are chosen as the product of an integer and $2\pi/L$ for periodic boundaries over a cubic region $L \times L \times L$. The present simulation periodic domain is taken as $15 \times 15 \times 15$ (in DPD units).

4.1 Spring model for suspended particles

The multiphase nature of the suspensions may be modelled by using more than one DPD species. In the spring model [12], a suspended particle is represented by a set of p basic DPD particles (p is small) that are connected, through stiff springs, to some reference sites collectively moving as a rigid body. For example, a spherical particle can be modelled using 6 or 8 basic DPD particles with their reference sites at the vertices of either an octahedron or a cube, respectively. The shape and size of a suspended particle are actually defined by the repulsive force field generated by the constituent particles of a suspended particle (not by their locations).

The forces on constituent particles of the kth suspended particle are

$$\mathbf{F}_i^k(t) = \sum_{j=1, j\neq i}^{N} \left[\mathbf{F}_{ij,C}^k(t) + \mathbf{F}_{ij,D}^k(t) + \mathbf{F}_{ij,R}^k(t)\right] + \mathbf{F}_{i,S}^k(t), \quad i = (1, 2, \cdots, p), \tag{30}$$

where $\mathbf{F}_{i,S}^k(t) = -H\left[\mathbf{r}_i^k(t) - \overline{\mathbf{r}}_i^k(t)\right]$ is the spring force with H being the stiffness of the spring and $\overline{\mathbf{r}}_i^k(t)$ the position of the reference site.

It should be pointed out that the sum of the spring forces on the constituent particles of

the suspended particle has a zero mean. The reference sites are calculated through their Newton-Euler equations, using data from the previous time step, while the velocities of their associated DPD particles are found by solving the DPD equations at the current time step.

4.2 Finding a length scale introduced into the solvent system due to the presence of suspended particles

Three approaches are presented. In the first two, the mean distance between the suspended particles is taken as a new length scale to the solvent system. In the third approach, transverse-current autocorrelation functions (TCAFs) are used to estimate a new length scale.

4.2.1 Approach 1

A length scale that is introduced into the solvent system can be regarded as the mean distance between the suspended particles; a convenient distance is an estimate of a side of the cube of a particle,

$$\lambda = \frac{1}{n_c^{1/3}}, \tag{31}$$

where n_c is the number density of the colloidal (particulate) phase.

4.2.2 Approach 2

The mean inter-colloid distance is estimated as the radius of the sphere of the volume per particle (the Wigner-Seitz radius [19])

$$\lambda = \left(\frac{3}{4\pi n_c}\right)^{1/3}. \tag{32}$$

4.2.3 Approach 3: TCAF

Here, we propose a scheme, based on TCAFs, to estimate a length scale introduced into the solvent system from the spring constraints. For a given volume fraction of the suspended phase, two corresponding systems, containing all the solvent particles and the constituent particles of the suspended phase, are considered. Note that the solvent and the constituent particles are all subjected to the same DPD parameters, i.e. those defined in (29). In the first system, all the particles are acted on by DPD forces and are not under any other constraints. In the second system, some of the particles (constituent particles) are constrained by the springs to form suspended particles. The two systems are assumed to represent some simple fluids. Results concerning the dependence of the viscosity on the wave number (wavelength) by the TCAF approach for the two systems are shown Figure 2. Extrapolations are then conducted to obtain the viscosities in the hydrodynamic limit ($k \to 0$). Due to the presence of springs, an effective length scale of the constrained system is less than the side of the simulation box, and its viscosity is seen to be lower. The constrained system in the hydrodynamic limit can thus be considered as the free system at the wave number (wavelength) that corresponds to the hydrodynamic-limit viscosity of the constrained system. This wavelength is taken as a new length scale in the solvent phase.

Table 1 displays the effective wavelength of the solvent phase against the volume fraction of the suspended phase by the three approaches, while Table 2 details the corresponding effective wave numbers and effective viscosities in the TCAF case. Note that compressibility of the solvent is matched to that of water, i.e. $a_{ij} = 3.53$, and the simulation box is taken as $15 \times 15 \times 15$ (in DPD units).

4.3 Effect of the repulsion coefficient

It will be shown that the input repulsion strength can affect the system viscosity. In the present study, the input viscosity of the solvent phase is specified as 30. Water-compressibility matching leads to $a_{ij} = 3.53$. By simulating Couette flow (a non-equilibrium approach), the solvent's viscosity is estimated as 29.08, close to the input value. Increasing

a_{ij}, the solvent's viscosity is observed to have a larger value, e.g. (29.66, 30.22, 30.66) for $a_{ij} = (6.50, 9.50, 18.50)$, which correspond to a positive change of 1.99%, 3.92% and 5.45%, respectively. Increasing a_{ij} produces a less compressible fluid and is more effective in preventing particle overlap. However, at large values, the conservative force can be dominant and the DPD system has a solid-like behaviour (particles do not move, just oscillate about their positions). Here, we limit our attention to the change within about 2 %, where the diffusion coefficient is observed to stay constant at large times as shown in Figure 3.

4.4 Numerical results

Two solvent fluids with $a_{ij} = 3.53$ (water compressibility) and $a_{ij} = 6.50$ (a fluid less compressible than water) are considered. Their viscosities are estimated taking into account the finite-size effect due to the presence of the suspended particles. For the viscosity of the suspension, we are only interested in the value in the hydrodynamic limit ($k \to 0$). A simple shearing at a small Péclet number of 0.18 (non-equilibrium approach) is thus considered here as an efficient estimation. Note that the Péclet number (dimensionless shear rate) is defined as $Pe = \dot{\gamma}a^2/D_0$, where $\dot{\gamma}$ is the shear rate, a is the sphere radius and D_0 is the single-sphere diffusion coefficient. The viscosity is calculated from the xy component of the stress tensor (11), i.e. $\eta = \langle T_{xy} \rangle / \dot{\gamma}$.

Results concerning the dependence of reduced viscosity (η_r) on volume fraction (ϕ) are shown in Figure 4 for $a_{ij} = 3.53$ and in Figure 5 for $a_{ij} = 6.50$. The variation of the reduced viscosity can be divided into 3 regimes: dilute ($\phi \lesssim 0.02$), semi-dilute ($\phi \lesssim 0.25$) and concentrated ($\phi \gtrsim 0.25$). They are compared with the theoretical result in the dilute limit [20]

$$\eta_r = 1 + 2.5\phi, \tag{33}$$

and the well-known empirical result deduced from the optimisation of viscous energy dissipation [21]

$$\eta_r = \left(1 - \frac{\phi}{\phi_m}\right)^{-2}, \tag{34}$$

where ϕ_m is the random close-packing of monodisperse spheres. Here we take $\phi_m = 0.65$.

It can be seen that the original hydrodynamic DPD produces improved results with increasing repulsion strength a_{ij}. Viscosities with $a_{ij} = 6.50$ are noticeably larger than those with $a_{ij} = 3.53$ in the semi-dilute and concentrated regimes. However, their values are still much lower than those by the empirical relationship. At $\phi = 0.19$ (semi-dilute), the reduced viscosity is 1.59 for $a_{ij} = 3.53$, 1.78 for $a_{ij} = 6.50$ and 1.95 by the empirical result. At $\phi = 0.49$ (concentrated), the reduced viscosity is 5.17 for $a_{ij} = 3.53$, 6.69 for $a_{ij} = 6.50$ and 17.37 by the empirical result.

It can also be seen that the generalised hydrodynamic DPD in which a new length scale is estimated by means of TCAF yields a better behaviour than the original hydrodynamic DPD in all three regimes for both fluids considered. In the dilute limit, improved agreements with Einstein's relation are achieved. In the semi-dilute regime, visible higher-order effects are observed. In the concentrated regime, faster growths are obtained. At $\phi = 0.49$, the reduced viscosity is significantly increased from 5.17 to 9.69 in the case of $a_{ij} = 3.53$ and from 6.69 to 12.46 in the case of $a_{ij} = 6.50$. Furthermore, with a_{ij} increased from 3.53 to 6.50, a better agreement with the empirical relationship is also achieved with the proposed TCAF-DPD approach.

For the generalised hydrodynamic DPD approaches based on sphere/cube mean distance, it is observed that the reduced viscosity is overestimated in every case studied. The reason for this could be that their estimations of a new length scale do not take into account of the actual distribution of suspended particles (they are functions of the box volume and the number of suspended particles only as shown in (31) and (32)). In contrast, the proposed TCAF estimation of a new length scale relies not only on the number density of the colloidal phase but also on the locations and velocities of particles in the system at equilibrium. As a result, for systems having the same particle number density, the proposed estimation can lead to different results for the new length scale.

5 Concluding remarks

In this work, particulate suspensions are simulated with the dissipative particle dynamics (DPD) method, in which the spring model is used to model suspended particles. In estimating the solvent's viscosity, DPD is employed in its generalised hydrodynamic regime to take into account the finite size effect due to the presence of suspended particles. The effective sizes (wavelengths) are predicted by several approaches, and the transverse current autocorrelation functions (TCAFs) approach is shown to yield the most reasonable results. Improved reduced viscosities of the suspension are clearly observed in the dilute ($\phi \lesssim 0.02$, linear dependence), semi-dilute ($\phi \lesssim 0.25$, visible higher-order effects) and concentrated ($\phi \gtrsim 0.25$, rapid growth) regimes, compared to the theoretical dilute limit, and the best know empirical results at non-dilute regime. Further improvement can also be acquired by increasing the repulsion to an appropriate value, where the actual solvent viscosity in the hydrodynamic limit is still kept close to the input viscosity and the diffusion coefficient of the solvent still stays constant at large times.

References

1. N. Phan-Thien, N. Mai-Duy, Understanding Viscoelasticity: An Introduction to Rheology, third ed., Springer International Publishing, Cham, 2017.

2. J.P. Boon, S. Yip, Molecular Hydrodynamics, Dover Publications Inc, New York, 1991.

3. J.P. Hansen, I.R. McDonald, Theory of Simple Liquids, third ed., Academic Press, London, 2006.

4. M.B. Liu, G.R. Liu, L.W. Zhou and J.Z. Chang, Dissipative Particle Dynamics (DPD): An Overview and Recent Developments, Archives of Computational Methods in Engineering 22(4)(2015)529-556.

5. P. Español and P.B. Warren, Perspective: Dissipative particle dynamics, J. Chem. Phys. 146(2017)150901

6. T. Ye, D. Pan, C. Huang and M.B. Liu, Smoothed particle hydrodynamics (SPH) for complex fluid flows: Recent developments in methodology and applications, Physics of Fluids 31(1)(2019)011301

7. C. Marsh, Theoretical Aspects of Dissipative Particle Dynamics, Ph.d. thesis. University of Oxford, Oxford, 1998.

8. J.M.V.A. Koelman, P.J. Hoogerbrugge, Dynamic simulations of hard-sphere suspensions under steady shear, Europhysics Letters 21(3)(1993)363-368.

9. M. Whittle, K.P. Travis, Dynamic simulations of colloids by core-modified dissipative particle dynamics, J Chem Phys 132(2010)124906

10. S. Jamali, M. Yamanoi, J. Maia, Bridging the gap between microstructure and macroscopic behavior of monodisperse and bimodal colloidal suspensions, Soft Matter 9(2013)1506-1515.

11. W. Pan, B. Caswell, G.E. Karniadakis, Rheology, microstructure and migration in Brownian colloidal suspensions, Langmuir 26(1)(2010)133-142.

12. N. Phan-Thien, N. Mai-Duy, B.C. Khoo, A spring model for suspended particles in dissipative particle dynamics, Journal of Rheology 58(2014)839-867.

13. M. Ripoll, M.H. Ernst, P. Español, Large scale and mesoscopic hydrodynamics for dissipative particle dynamics, J Chem Phys 115(15)(2001)7271-7284.

14. N. Phan-Thien, N. Mai-Duy, T.Y.N. Nguyen, A note on dissipative particle dynamics (DPD) modelling of simple fluids, Computers and Fluids 176(2018)97-108.

15. N. Mai-Duy, N. Phan-Thien, T. Tran-Cong, An improved dissipative particle dynamics scheme, Appl Math Model 46(2017)602-617.

16. N. Mai-Duy, N. Phan-Thien, T. Tran-Cong, Imposition of physical parameters in dissipative particle dynamics, Comput Phys Comm 221(2017)290-298.

17. N. Mai-Duy, N. Phan-Thien, B.C. Khoo, Investigation of particles size effects in Dissipative Particle Dynamics (DPD) modelling of colloidal suspensions, Comput Phys Comm 189(2015)37-46

18. R.D. Groot, P.B. Warren, Dissipative particle dynamics: bridging the gap between atomistic and mesoscopic simulation, J Chem Phys 107(1997)442335.

19. L. Girifalco, Statistical Mechanics of Solids, Oxford University Press, Oxford, 2000.

20. A. Einstein, Eine neue bestimmung der moleküldimensionen, Ann. der Phys. 14(2005)229-247 [Reprinted in Investigations on the Theory of the Brownian Movement, edited by R. Furth, translated by A.D. Cowper, Dover, New York, 1956].

21. D. Quemada, Rheology of concentrated disperse systems and minimum energy dissipation principle, Rheol. Acta 16(1) (1977) 8294.

Table 1: Effective wavelength of the solvent phase against volume fraction of the suspended phase by the three approaches. Compressibility of the solvent is matched to that of water, i.e. $a_{ij} = 3.53$, and the simulation box is taken as $15 \times 15 \times 15$ (in DPD units).

	Effective wavelengths		
ϕ	Sphere-based mean distance	Cube-based mean distance	TCAF
0.0119	3.1018	5.0000	12.8671
0.0277	2.3263	3.7500	9.4465
0.0526	1.8611	3.0000	5.3996
0.0876	1.5509	2.5000	4.7463
0.1323	1.3293	2.1429	3.8475
0.1854	1.1632	1.8750	3.2045
0.2447	1.0339	1.6667	2.7583
0.3077	0.9305	1.5000	2.4303
0.3717	0.8459	1.3636	2.1586
0.4344	0.7754	1.2500	1.9544
0.4940	0.7158	1.1538	1.7431

Table 2: Effective wave number, wavelength and viscosity of the solvent phase against volume fraction of the suspended phase by the TCAF approach. Compressibility of the solvent is matched to that of water, i.e. $a_{ij} = 3.53$, and the simulation box is taken as $15 \times 15 \times 15$ (in DPD units).

ϕ	Effective k	Effective λ	Effective η
0.0119	0.4883	12.8671	28.9109
0.0277	0.6651	9.4465	28.7144
0.0526	1.1636	5.3996	27.2179
0.0876	1.3238	4.7463	26.5560
0.1323	1.6331	3.8475	25.2043
0.1854	1.9608	3.2045	23.8032
0.2447	2.2779	2.7583	22.3348
0.3077	2.5853	2.4303	20.7466
0.3717	2.9108	2.1586	18.9952
0.4344	3.2149	1.9544	17.4017
0.4940	3.6047	1.7431	15.5091

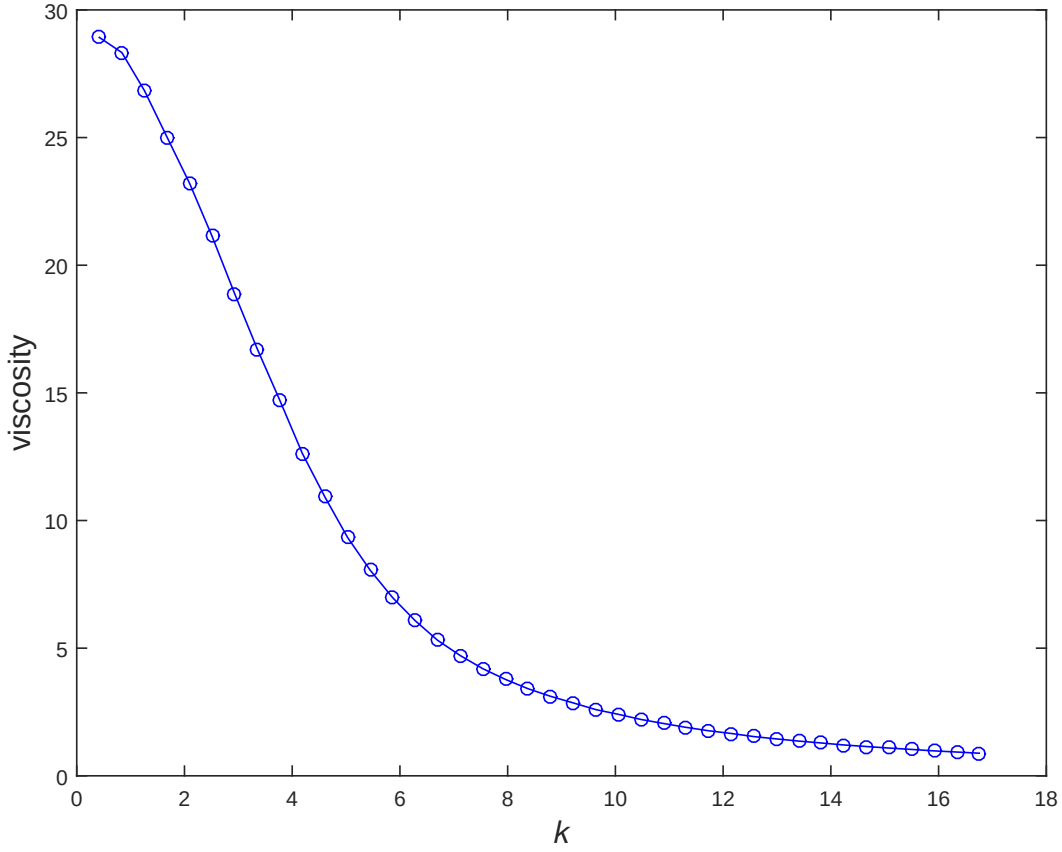

Figure 1: Solvent phase ($a_{ij} = 3.53$ (water compressibility), $n = 4, m = 1, k_BT = 1, r_c = 1.5, \eta = 30, S_c = 500$): the viscosity is a decreasing function of the wave number k (or an increasing function of the wavelength $\lambda = 2\pi/k$).

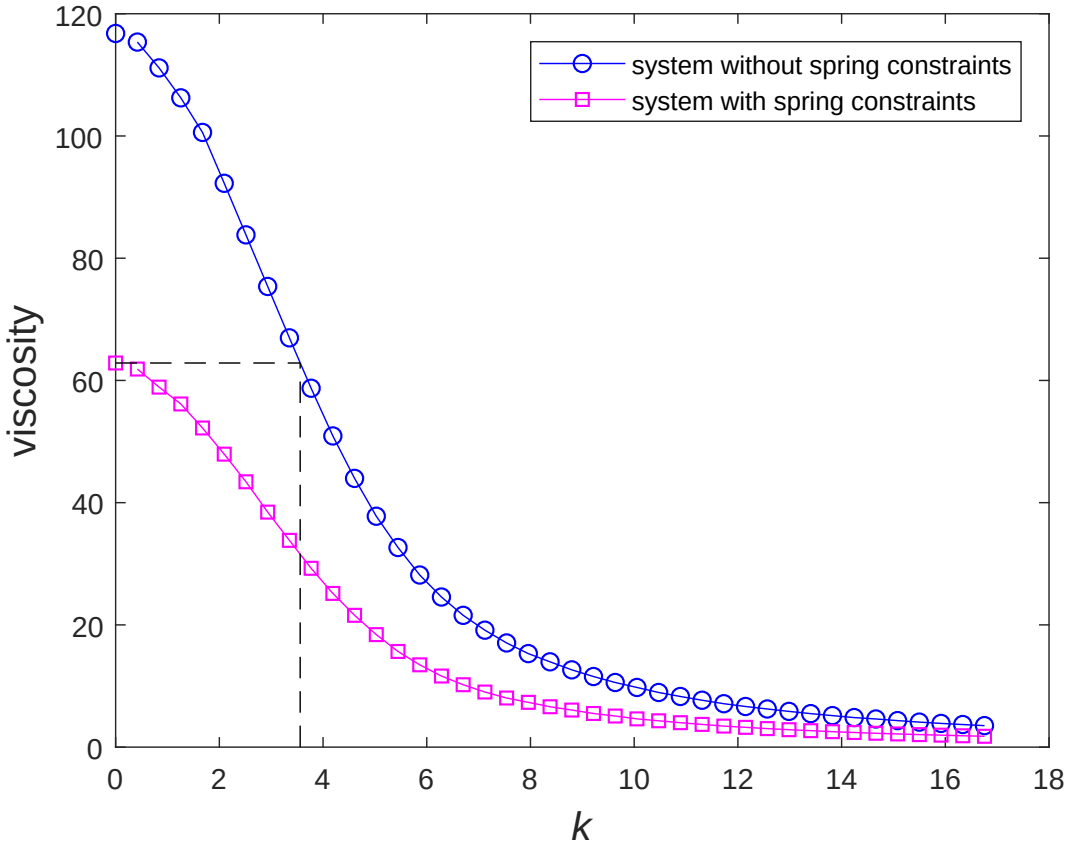

Figure 2: Process of finding a new length scale that is introduced into the solvent system due to the presence of suspended particles. For a given volume fraction, two corresponding systems (one without any spring constraints and the other with some spring constraints as a model for suspension) are considered; they have the same total numbers of the base particles and employ the same associated DPD parameters. The two systems are assumed to represent simple fluids; through the TCAF approach, their viscosities are shown to depend on the wave numbers (wavelengths). Extrapolations are then conducted to obtain the viscosities in the hydrodynamic limit ($k \to 0$). With springs, the effective length scale of the constrained system is less than the system size L, and its viscosity is seen to be lower. The constrained system in the hydrodynamic limit can be considered as the free system at the wave number (wavelength) that corresponds to the hydrodynamic-limit viscosity of the constrained system. This wavelength is taken as a new length scale in the solvent phase.

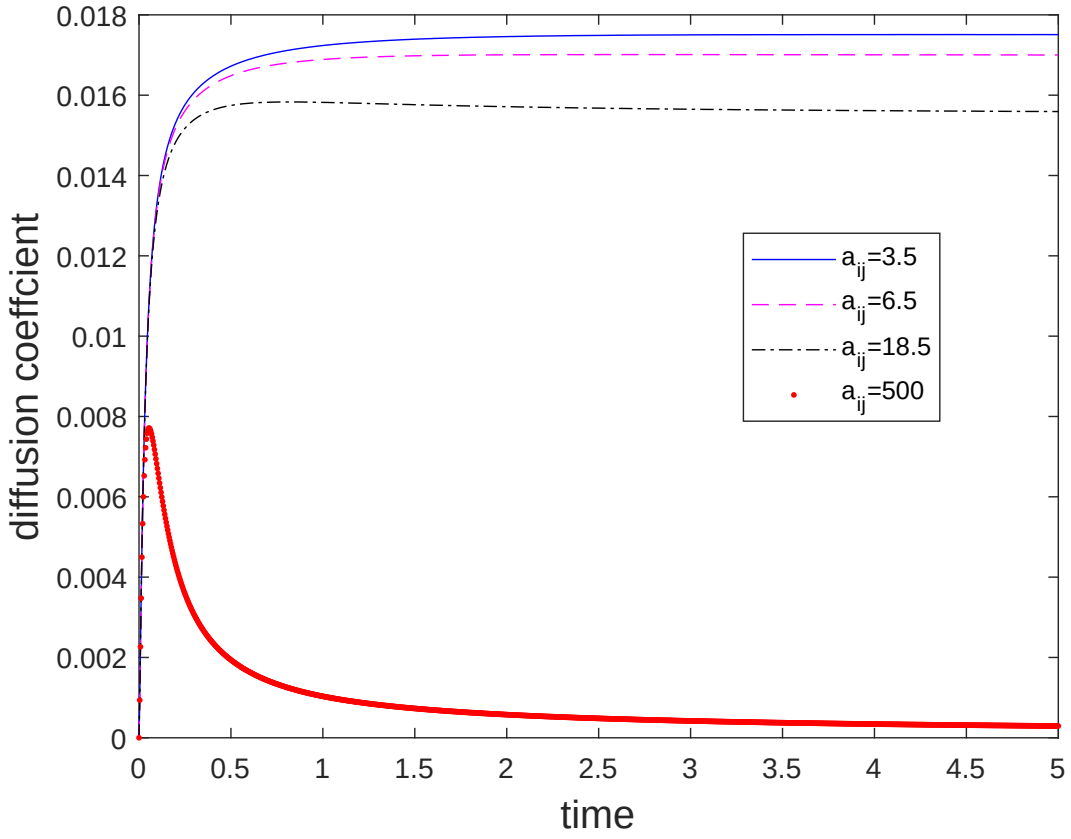

Figure 3: Diffusion coefficient against time for several values of the repulsion. For $a_{ij} = (3.53, 6.50)$, the diffusion coefficients are observed to stay constant at large times. For larger a_{ij}, there is some reduction in the coefficient and no significant diffusion at $a_{ij} = 500$.

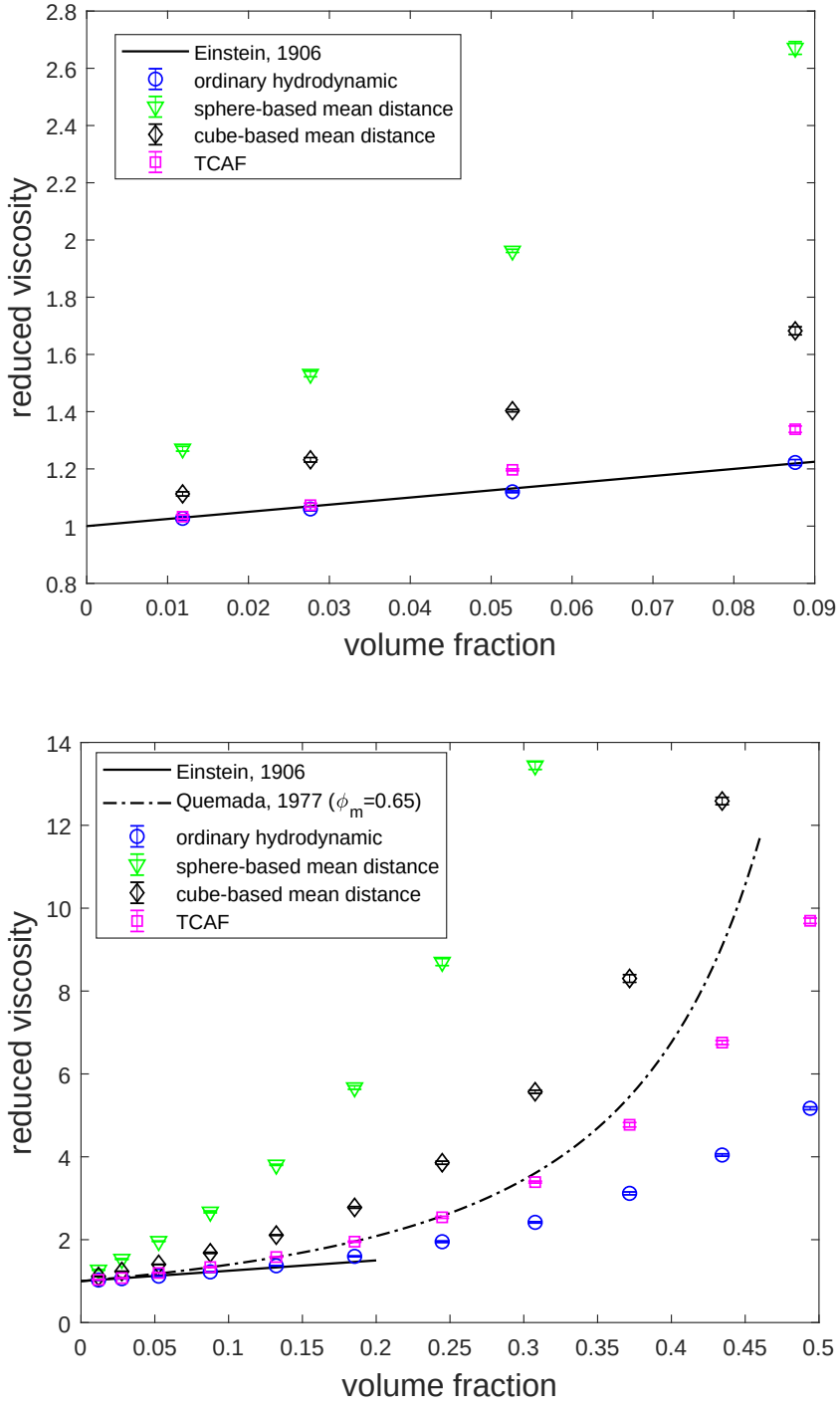

Figure 4: Reduced viscosity by original and generalised hydrodynamic DPD using the same repulsion $a_{ij} = 3.53$ (water compressibility). The latter (TCAF) is seen to have a better performance than the former in the dilute ($\phi \lesssim 0.02$, linear dependence), semi-dilute ($\phi \lesssim 0.25$, visible higher-order effects) and concentrated ($\phi \gtrsim 0.25$, rapid growth) regimes. It appears that the generalised hydrodynamic DPD based on sphere/cube mean distance overestimates the reduced viscosity in every regime. Theoretical results in the dilute regime [20] and empirical results [21], which have found widespread application, are also included for comparison purposes.

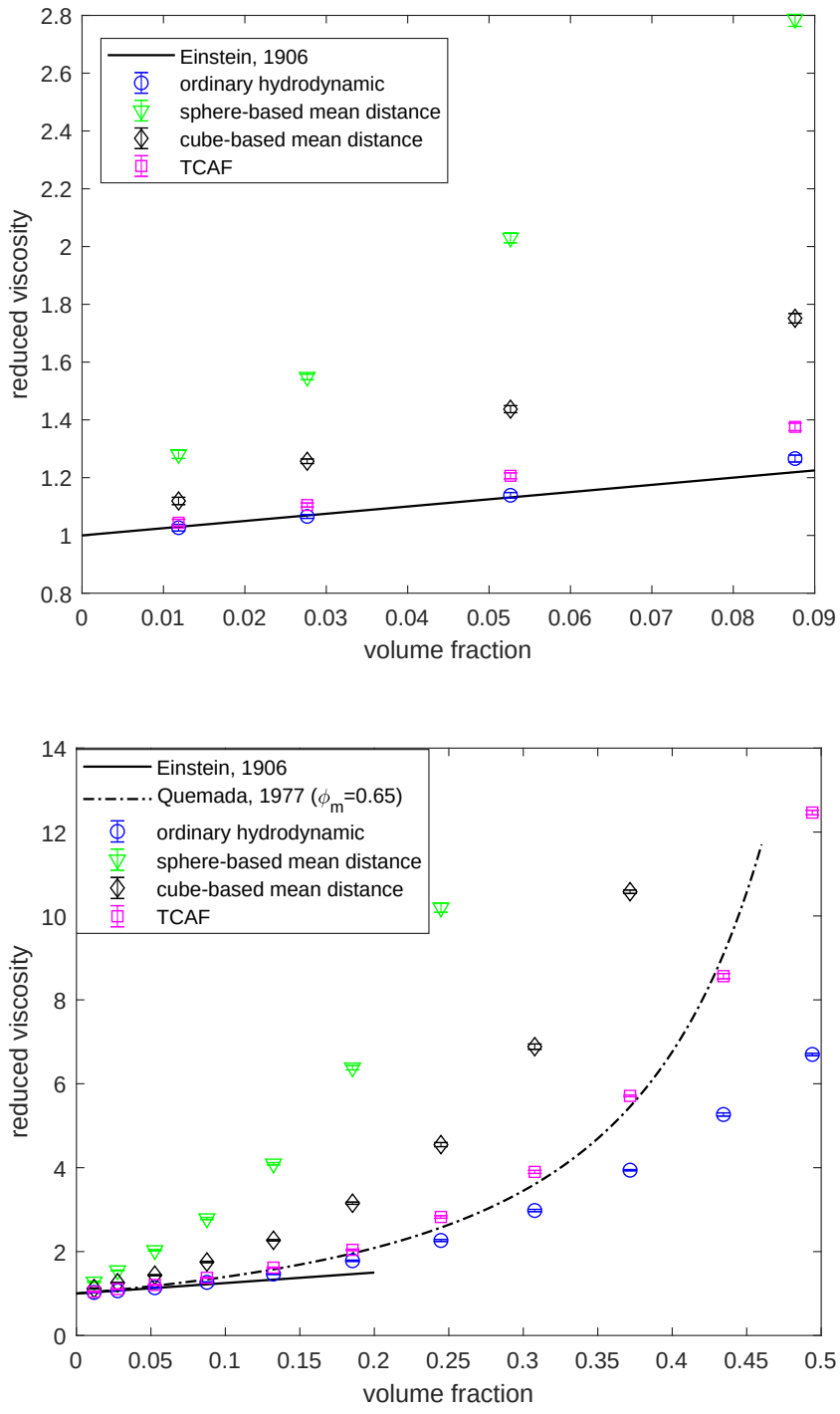

Figure 5: Reduced viscosity by original and generalised hydrodynamic DPD using the same repulsion $a_{ij} = 6.50$ (a fluid is less compressible than water). The latter (TCAF) is seen to have a better performance than the former in the dilute ($\phi \lesssim 0.02$, linear dependence), semi-dilute ($\phi \lesssim 0.25$, visible higher-order effects) and concentrated ($\phi \gtrsim 0.25$, rapid growth) regimes. It appears that the generalised hydrodynamic DPD based on sphere/cube mean distance overestimates the reduced viscosity in every regime. Theoretical results in the dilute regime [20] and empirical results [21], which have found widespread application, are also included for comparison purposes.